Chiral Nanotubes

Deutsche Ausgabe: DOI: 10.1002/ange.201602819
Internationale Ausgabe: DOI: 10.1002/anie.201602819

Fabrication of Chiral-Selective Nanotubular Heterojunctions through Living Supramolecular Polymerization

Xiaojie Ma, Yibin Zhang, Yifan Zhang, Yin Liu, Yanke Che, and Jincai Zhao*

Abstract: *Novel, chiral-selective linear nanotubular heterojunctions were achieved by living supramolecular polymerization of perylenediimide (PDI) derivatives. We demonstrate that the chiral seed can effectively bias achiral PDI molecules to polymerize on its ends in the identical helical sense. More interestingly, the chiral seed can bias the opposite enantiomers to grow expitaxially from its ends even in excess amounts relative to the seed. Furthermore, we demonstrate that the biasing effect of the chiral seed on the opposite enantiomer is not dependent on the length of the chiral seed but is related to the intrinsic length of the elongated nanotube from the opposite enantiomer. The fabrication of chiral-selective nanotubes was achieved by application of the unique biasing effect of the chiral seed in living supramolecular self-assembly.*

In recent years, living supramolecular polymerization has emerged as a powerful technique for the generation of complex architectures with programmable and precisely controlled dimensions.[1–14] For example, Manners et al. have pioneered the fabrication of block polymers (for example, polyferrocenylsilane, PFS) into various elaborate nanoscale architectures via living crystallization-driven self-assembly.[1–5] However, in comparison to their polymer counterparts, small organic molecules were only recently reported to undergo living self-assembly in 2014. Takeuchi and co-workers first reported rationally designed porphyrin-based monomers undergoing living supramolecular polymerization.[6] The main challenge in the living assembly of common small molecules lies in the insufficient energy barrier for the initial nucleation process, which results in spontaneous nucleation that competes with the crystallization-driven elongation process. To address this challenge, control over the pathway complexity (for example, the application of kinetically trapped off-pathway assemblies to inhibit the initial nucleation) has emerged as an effective approach for living self-assembly.[6,10,15–17] Despite examples being sparsely reported in this research area,[6,8,10,18] the living assembly of small molecules continues to lag far behind that of their polymer counterparts and has not been applied to create complex functional architectures (for example, chiral heterogeneous supramolecular structures) that are difficult to access by common self-assembly methods. Recently, Aida and co-workers reported the achievement of the helix sense-selective supramolecular polymerization by using one-handed nanotube as a seed.[19] This result inspired us to explore the possibility of constructing chiral-selective supramolecular architectures via living self-assembly. Because living small molecule self-assembly requires no specific solution processing (for example, dilution or heating) to prevent spontaneous aggregation of the second monomer compared to common seeded self-assembly,[19,20] this approach should provide a more convenient and powerful method of fabricating unprecedented chiral-selective supramolecular heterojunctions.

Herein, new chiral-selective linear heterogeneous nanotubes were prepared by living supramolecular self-assembly of perylenediimide (PDI) derivatives (Figure 1 a). We demonstrate that the chiral nanotube seed induced the polymerization of achiral PDI molecule **2** at the seed ends in the same helical sense (Figure 1 b), which is analogous to the sergeants-and-soldiers effect in molecular self-assembly.[21–31] More interestingly, the chiral seed is capable of biasing the opposite enantiomer in excess amounts (for example, 2–4-fold relative to the seed) to polymerize in the same helical sense at its ends, which surprisingly disregards the majority rule that was well recognized in molecular self-assembly.[23,26,28,30,32–34] Furthermore, we demonstrate that the biasing effect of the chiral seed on the opposite enantiomer is not dependent on the seed length of the chiral seed but is instead related to the intrinsic length of the elongated nanotube from the opposite enantiomer. When the length of the elongated nanotube from the opposite enantiomer was larger than a certain value (ca. 1.2 μm in this study), the seed-initiated helical sense of the nanotubular heterojunction was eventually inverted. Therefore, the unique biasing effect of the chiral seed in the living self-assembly can be used to fabricate chiral-selective architectures from the enantiomers.

The monomers selected in this study were PDI derivatives (Figure 1 a). We previously reported that the self-assembly of these molecules follows two aggregation pathways, where the off-pathway microribbons quickly formed prior to the formation of the on-pathway nanotubes.[35] After careful examination of the time-dependent fluorescence intensity of the microribbons at 595 nm, a sharp decrease in the fluorescence intensity was observed at 24 h, which is characteristic of an autocatalytic process involving microribbon decomposition (Supporting Information, Figure S1). This result motivated us to explore the possibility of the living supramolecular assembly of these molecules. Prior to the experiments, we prepared the seeds of **1** and **2** by ultrasonicating the

[*] X. Ma, Y. Zhang, Y. Zhang, Y. Liu, Prof. Dr. Y. Che, Prof. Dr. J. Zhao
Key Laboratory of Photochemistry, Institute of Chemistry
Chinese Academy of Sciences, Beijing 100190 (China)
and
University of Chinese Academy of Sciences
Beijing 100049 (China)
E-mail: ykche@iccas.ac.cn

Supporting information for this article can be found under: http://dx.doi.org/10.1002/anie.201602819.

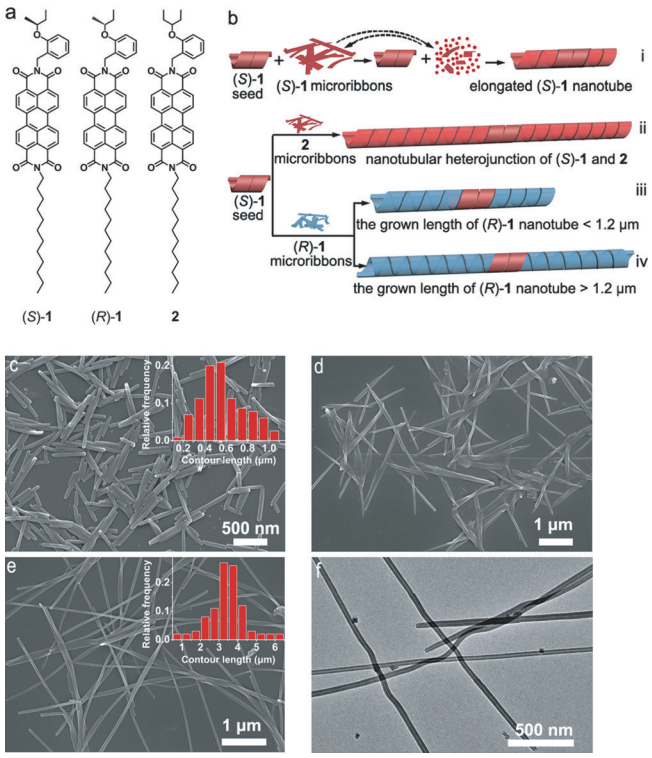

Figure 1. a) Molecular structures of molecules **1** and **2**. b) Illustration of the living supramolecular polymerization process of (*S*)-**1** (i) and the formation of nanotubular heterojunctions via living supramolecular polymerization of **1** and **2** (ii–iv). c) SEM image of (*S*)-**1** seeds obtained through ultrasonication. Inset: length distribution of (*S*)-**1** seeds (the lengths of more than 100 nanotubes were measured). d) SEM image of the aggregates formed 2 h after the living assembly in which (*S*)-**1** seeds were added to the stock solution of (*S*)-**1** microribbons at a molar ratio of 1:5. e) SEM and f) TEM images of the aggregates formed 20 h after the same living assembly. Inset in (e): length distribution of the formed nanotubular heterojunctions at 20 h after the living assembly.

corresponding prefabricated nanotubes at −70 °C for 1 h. Analysis of the length of more than 100 seeds using scanning electron microscopy (SEM) and transmission electron microscopy (TEM) revealed that the resulting nanotube seeds ranged in length from 0.2 to 1 μm (Figure 1c; Supporting Information, Figure S2).

Upon the addition of (*S*)-**1** seeds (0.003 μmol, 0.5 mL) to the prefabricated stock solution of (*S*)-**1** microribbons[35] (0.015 μmol, 2.5 mL) in a chloroform/ethanol mixture (volume ratio: 1:15), the living nature of the seeded self-assembly was investigated by SEM and TEM. As shown in Figure 1 and the Supporting Information, Figure S3, the nanotubes became elongated with time progress and simultaneously the microribbons became smaller and fewer, revealing that the gradual disassembly of the microribbons and the growth of the nanotubes. After 20 h of self-assembly, substantially elongated aggregates were formed, accompanied by the disappearance of the precursor microribbons (Figure 1e; Supporting Information, Figure S4). Our TEM observations confirmed the nanotubular structure of the elongated aggregates (Figure 1f) similar to that of the seeds. Furthermore, the resulting nanotubes have approximately six times the length of the seed (Figure 1e), which is indicative of the epitaxial growth of the monomers on the ends of the seeds. The living nature of the seeded self-assembly was further supported by optical characterizations. As shown in the Supporting Information, Figure S5a,c, the fluorescence intensity of the microribbons began to decrease quickly, without a lag time, after the seed was added; this behavior contrasts sharply with the invariable fluorescence intensity of the microribbons in the absence of the seeds (Supporting Information, Figure S5b). Likewise, a new absorption band centered at 555 nm, which corresponds to the formation of nanotubes,[35] emerged within 2 h after the addition of the seeds into the microribbons solution (Supporting Information, Figure S6a); by contrast, the absorption spectra of the microribbons solution without seed addition remained unchanged (Supporting Information, Figure S6b). These results strongly indicate that the added seeds induced the rapid decomposition of the metastable microribbons, which, in turn, induced the resulting monomers to grow on both ends. This result demonstrates the living nature of the self-assembly of (*S*)-**1**, as illustrated in Figure 1b. Notably, the helical molecular packing of the elongated portion is identical to that of the seed, as confirmed by the circular dichroism (CD) spectra, in which the same positive Cotton effect between 470 nm and 650 nm increased with elongation of the resulting nanotubes (Supporting Information, Figure S6c). Furthermore, molecules (*R*)-**1** and **2** were capable of functioning as seeds to initiate the living self-assembly (Supporting Information, Figures S7 and S8).

We envisioned that the living nature of the self-assembly of these molecules may enable the generation of various nanotubular heterojunctions by recruiting another monomer to epitaxially grow in the same fashion as the block polymers. To investigate this hypothesis, we added (*S*)-**1** seeds with different molar ratios to the stock solution of **2** microribbons that were obtained after 2 h of self-assembly according to a previously reported approach,[35] and monitored the time-dependent fluorescence of the microribbons. After the addition of (*S*)-**1** seeds, the fluorescence of the microribbons immediately decreased, without a lag time (Figure 2a; Supporting Information, Figure S9), which suggests the growth of nanotubular assemblies from monomers resulting from immediate disassembly of the metastable microribbons. This process was further evidenced by SEM measurements where the nanotubes epitaxially elongated with time progress and the microribbons simultaneously became smaller and fewer (Supporting Information, Figure S10). A high-magnification TEM image revealed that the diameter of the grown tubular segment is slightly smaller than that of the seed, indicative of the heterojunction structure (Supporting Information, Figure S11). After 20 h of self-assembly, the **2** microribbons completely disappeared and only the elongated nanotubes were observed (Figure 2b–d; Supporting Information, Figure S12). Furthermore, with the molar ratio of (*S*)-**1** seeds to **2** microribbons at 1:1, 1:5, and 1:10, the resulting nanotubes have approximately 2, 6, and 11 times the length of the seeds, respectively (Supporting Information, Figure S13), indicating the living supramolecular polymerization of **2** monomers on the ends of the seeds. Likewise, the nanotubular heterojunctions were formed using **2** nanotubes as the seed

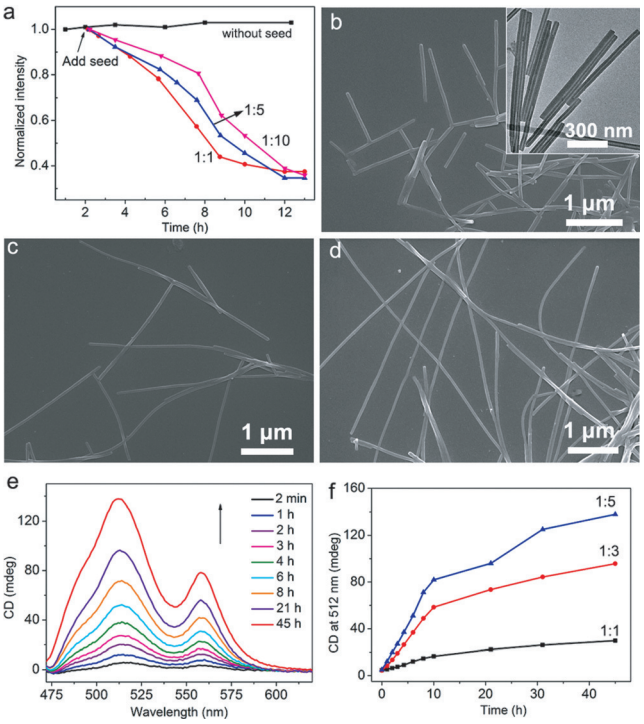

Figure 2. a) Time-dependent changes in the fluorescence intensity at 595 nm, which was assigned to **2** microribbons (0.0125 μmol) in a chloroform/ethanol mixture (2 mL), upon addition of (*S*)-**1** seeds (0.0125, 0.0025, and 0.0012 μmol) at molar ratios of 1:1, 1:5, and 1:10 relative to **2** microribbons and without the addition of (*S*)-**1** seeds. Data error ±10%. b)–d) SEM images of the nanotubular heterojunctions formed 20 h after the living assembly in which (*S*)-**1** seeds were added to the stock solution of **2** microribbons at molar ratios of 1:1 (b), 1:5 (c), and 1:10 (d). Inset in (b): TEM image of the formed nanotubular heterojunctions. e) Time-dependent changes in the CD spectra of the aggregates upon addition of (*S*)-**1** seeds (0.003 μmol, 0.5 mL) into **2** microribbons (0.015 μmol) in a chloroform/ethanol mixture (2.5 mL) at a molar ratio of 1:5. f) Time-dependent CD signals at 512 nm upon addition of (*S*)-**1** seeds (0.003 μmol, 0.5 mL) into **2** microribbons (0.003, 0.009, and 0.015 μmol) in a chloroform/ethanol mixture (2.5 mL) at molar ratios of 1:1, 1:3, and 1:5. Data error ±10%.

and the metastable microribbons of (*S*)-**1** as the stock material (Supporting Information, Figures S14 and S15). Because the seeds that consist of (*S*)-**1** are chiral, the growth of achiral **2** on the chiral seed was expected to adopt the same helical sense. Indeed, as shown in Figure 2e, the CD spectral profile exhibited a positive Cotton effect between 470 nm and 650 nm (assignable to the seeds) that increased substantially with elongation of the nanotubes, indicating that the (*S*)-**1** seeds initiated the epitaxial growth of achiral **2** monomers in the same helical sense. The biasing effect of the chiral seeds on the molecular packing of **2** monomers was further confirmed by the CD intensity of the resulting nanotubes being approximately proportional to the amount of **2** microribbons and the seeds (Figure 2f; Supporting Information, Figure S16). Here, the biasing effect of the seed on the achiral **2** resembles the common sergeants-and-soldiers effect in molecular self-assembly.[21–31]

These results further motivated us to investigate if the chiral seeds are capable of initiating the supramolecular polymerization of the opposite enantiomer on their ends and simultaneously biasing the opposite enantiomer to adopt packing in the same helical sense. After (*S*)-**1** seeds of ca. 600 nm in length were added to the stock solution of (*R*)-**1** microribbons obtained after 2 h of self-assembly according to a previously reported method, elongated nanotubes were formed after self-assembly (Figure 3; Supporting Information, Figure S17). The heterojunction structure consists of the grown tubular segment from (*R*)-**1** with a smaller diameter and the seed segement was clearly imaged in high-magnification TEM images (Supporting Information, Figure S18). Furthermore, with the molar ratio of (*R*)-**1** microribbons to (*S*)-**1** seeds at 1:1, 1:2, 1:3, and 1:5, the resulting nanotubes have about 2, 3, 4, and 6 times the length of the seeds, respectively, indicating the living polymerization of (*R*)-**1** on the ends of (*S*)-**1** seeds.

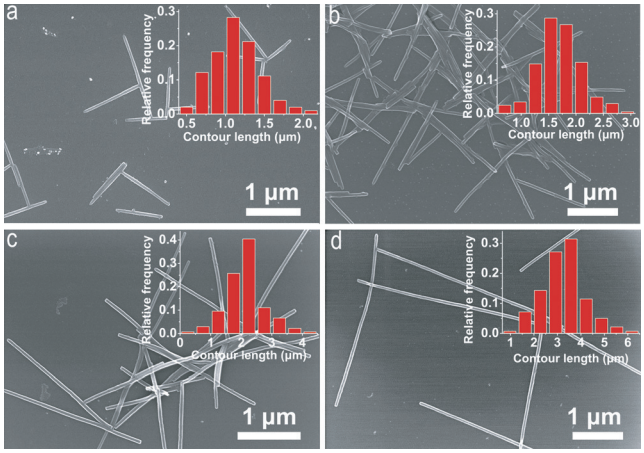

Figure 3. SEM images of the nanotubular heterojunctions that were formed 20 h after beginning the living assembly where (*S*)-**1** seeds (0.003 μmol, 0.5 mL) were added to the stock solution of (*R*)-**1** microribbons (0.003, 0.006, 0.009, and 0.015 μmol) in a chloroform/ethanol mixture (2.5 mL) at molar ratios of 1:1 (a), 1:2 (b), 1:3 (c), and 1:5 (d). Insets: length distribution of the formed nanotubular heterojunctions at 20 h after beginning the living assembly (more than 100 nanotubes were measured).

Interestingly, the CD signals became more intense with time progress when the molar ratio of the amount of (*R*)-**1** to that of (*S*)-**1** seed (ca. 600 nm in length) was even 2, (Figure 4a,b), confirming that the helical sense of the newly grown nanotube from (*R*)-**1** is identical to that of the seed. This result is surprising because it disregards the majority rule generally recognized in the molecular self-assembly of enantiomers.[23,26,28,30,32–34] Notably, when the amount of (*R*)-**1** relative to that of (*S*)-**1** was further increased (for example, 3:1 and 5:1), the CD bands increased initially and then decreased gradually to a negative Cotton effect (Figure 4b,c; Supporting Information, Figure S19). This results indicate that more (*R*)-**1** monomers can only be kinetically induced to take the same helical sense to the seed; they would further transform to a thermodynamically stable form; that is, the stereochemically identical packing. This observation also

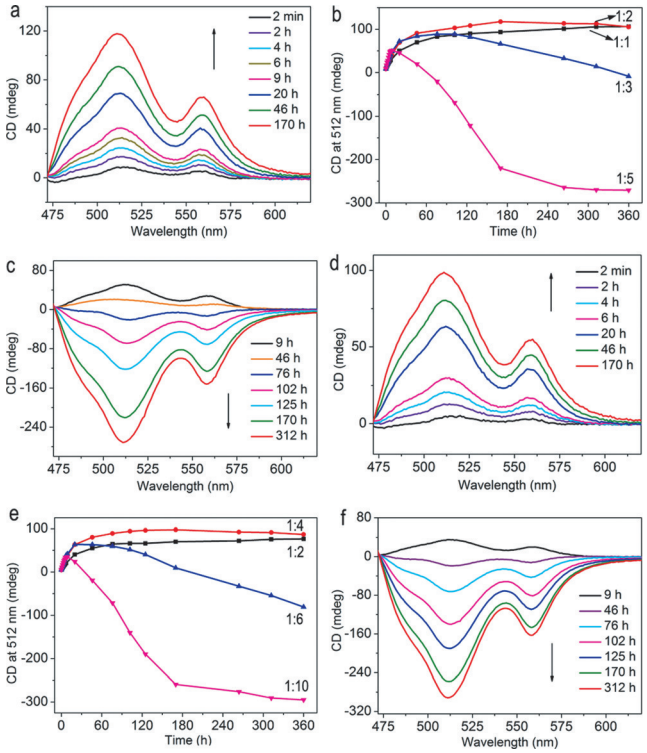

Figure 4. a) Time-dependent changes in the CD spectra of the aggregates upon addition of (*S*)-**1** seeds with a length of ca. 600 nm (0.003 μmol, 0.5 mL) to (*R*)-**1** microribbons (0.006 μmol) in a chloroform/ethanol mixture (2.5 mL). b) Time-dependent CD signals at 512 nm upon addition of (*S*)-**1** seeds with a length of ca. 600 nm (0.003 μmol, 0.5 mL) to (*R*)-**1** microribbons in a chloroform/ethanol mixture (2.5 mL) at molar ratios of 1:1, 1:2, 1:3, and 1:5. Data error ±10%. c) Time-dependent changes in the CD spectra of the aggregates upon addition of (*S*)-**1** seeds with a length of ca. 600 nm (0.003 μmol, 0.5 mL) to (*R*)-**1** microribbons (0.015 μmol) in a chloroform/ethanol mixture (2.5 mL). d) Time-dependent changes in the CD spectra of the aggregates upon addition of (*S*)-**1** seeds with a length of ca. 300 nm (0.0015 μmol, 0.5 mL) into (*R*)-**1** microribbons (0.006 μmol) in a chloroform/ethanol mixture (2.5 mL). e) Time-dependent CD signals at 512 nm upon addition of (*S*)-**1** seeds with a length of ca. 300 nm (0.0015 μmol, 0.5 mL) to (*R*)-**1** microribbons in chloroform/ethanol mixture (2.5 mL) at molar ratios of 1:2, 1:4, 1:6, and 1:10. Data error ±10%. f) Time-dependent changes in the CD spectra of the aggregates upon addition of (*S*)-**1** seeds with a length of ca. 300 nm (0.0015 μmol, 0.5 mL) to (*R*)-**1** microribbons (0.015 μmol) in a chloroform/ethanol mixture (2.5 mL).

suggests that the biasing effect of the chiral seeds decreased with elongation of the nanotube of the opposite enantiomer; consequently, the majority rule eventually took control, resulting in a negative Cotton effect. To gain additional insight into the biasing effect of the chiral seeds, we shortened the length of the chiral (*S*)-**1** seeds to ca. 300 nm by extending the ultrasound treatment time (Supporting Information, Figure S20) and evaluated their biasing effect on the supramolecular polymerization of the opposite enantiomer. Upon addition of half of the amount of (*S*)-**1** seeds with a length of ca. 300 nm relative to those that were ca. 600 nm in length (that is, keeping the same amount of active seed ends) to the previously described microribbon suspension, the short seeds biased the same amount of the opposite enantiomers (the molar ratio of (*R*)-**1** to that of (*S*)-**1** seeds is actually 4 in this case) to grow in the same sense (Figure 4d,e; Supporting Information, Figure S21). Likewise, more (*R*)-**1** grown on the seed kinetically maintained the same sense to the seed and then inverted gradually, as evidenced by time-dependent CD spectra (Figure 4e,f; Supporting Information, Figures S21 and S22). The similar biasing behaviors of these two types of seeds (Figure 4) indicate that the biasing effect of the chiral seed on the opposite enantiomer is not dependent on the length of the chiral seed but is related to the intrinsic length of the elongated nanotube from the opposite enantiomer (ca. 1.2 μm). Because the opposite enantiomers tend to adopt a stereochemically identical packing, we postulate that the observed chirality inversion is due to the enthalpy penalty that increases as the length of the elongated nanotube increases. A detailed mechanistic investigation is currently underway in our lab. Herein, we highlight that the fabrication of chiral-selective architectures from the enantiomers by application of a unique biasing effect of the chiral seed in the living supramolecular self-assembly.

In conclusion, we prepared new chiral-selective nanotubular heterojunctions via living supramolecular self-assembly. We demonstrated that the chiral nanotube seed not only induced the polymerization of an achiral PDI molecule at the seed ends in the same helical sense, but also initiated the polymerization of the opposite enantiomer even in excess amounts at the seed ends in the same helical sense. We further demonstrated that the biasing effect of the chiral seed on the opposite enantiomer is not dependent on the seed length of the chiral seed but related to the intrinsic length of the elongated nanotube from the opposite enantiomer. When the length of the elongated nanotube from the opposite enantiomer was larger than a certain value (ca. 1.2 μm in this study), the seed-induced helical sense of the nanotubular heterojunction eventually inverted. Therefore, the application of living supramolecular self-assembly provides a new approach for the preparation of chiral-selective nanostructures.

Acknowledgements

This work was supported by 973 project (No. 2013CB632405), NSFC (Nos. 21221002, 21322701, 21577147 and 21590811), the "Strategic Priority Research Program" of the CAS (No. XDA09030200) and the "Youth 1000 Talent Plan" Fund.

Keywords: chirality · nanotubes · pathway complexity · perylenediimide · supramolecular polymerization

How to cite: *Angew. Chem. Int. Ed.* **2016**, *55*, 9539–9543
Angew. Chem. **2016**, *128*, 9691–9695

[1] T. Gadt, N. S. Ieong, G. Cambridge, M. A. Winnik, I. Manners, *Nat. Mater.* **2009**, *8*, 144–150.
[2] J. B. Gilroy, T. Gädt, G. R. Whittell, L. Chabanne, J. M. Mitchels, R. M. Richardson, M. A. Winnik, I. Manners, *Nat. Chem.* **2010**, *2*, 566–570.
[3] Z. M. Hudson, C. E. Boott, M. E. Robinson, P. A. Rupar, M. A. Winnik, I. Manners, *Nat. Chem.* **2014**, *6*, 893–898.

[4] X. Wang, G. Guerin, H. Wang, Y. Wang, I. Manners, M. A. Winnik, *Science* **2007**, *317*, 644 – 647.
[5] P. A. Rupar, L. Chabanne, M. A. Winnik, I. Manners, *Science* **2012**, *337*, 559 – 562.
[6] S. Ogi, K. Sugiyasu, S. Manna, S. Samitsu, M. Takeuchi, *Nat. Chem.* **2014**, *6*, 188 – 195.
[7] M. Colomb-Delsuc, E. Mattia, J. W. Sadownik, S. Otto, *Nat. Commun.* **2015**, *6*, 7427 – 7434.
[8] A. Pal, M. Malakoutikhah, G. Leonetti, M. Tezcan, M. Colomb-Delsuc, V. D. Nguyen, J. van der Gucht, S. Otto, *Angew. Chem. Int. Ed.* **2015**, *54*, 7852 – 7856; *Angew. Chem.* **2015**, *127*, 7963 – 7967.
[9] J. W. Sadownik, E. Mattia, P. Nowak, S. Otto, *Nat. Chem.* **2016**, *8*, 264 – 269.
[10] A. Aliprandi, M. Mauro, L. De Cola, *Nat. Chem.* **2016**, *8*, 10 – 15.
[11] D. van der Zwaag, T. F. A. de Greef, E. W. Meijer, *Angew. Chem. Int. Ed.* **2015**, *54*, 8334 – 8336; *Angew. Chem.* **2015**, *127*, 8452 – 8454.
[12] R. D. Mukhopadhyay, A. Ajayaghosh, *Science* **2015**, *349*, 241 – 242.
[13] E. Mattia, S. Otto, *Nat. Nanotechnol.* **2015**, *10*, 111 – 119.
[14] A. Jain, S. J. George, *Mater. Today* **2015**, *18*, 206 – 214.
[15] P. A. Korevaar, S. J. George, A. J. Markvoort, M. M. J. Smulders, P. A. J. Hilbers, A. P. H. J. Schenning, T. F. A. De Greef, E. W. Meijer, *Nature* **2012**, *481*, 492 – 496.
[16] S. Ogi, T. Fukui, M. L. Jue, M. Takeuchi, K. Sugiyasu, *Angew. Chem. Int. Ed.* **2014**, *53*, 14363 – 14367; *Angew. Chem.* **2014**, *126*, 14591 – 14595.
[17] S. Ogi, V. Stepanenko, J. Thein, F. Würthner, *J. Am. Chem. Soc.* **2016**, *138*, 670 – 678.
[18] M. E. Robinson, D. J. Lunn, A. Nazemi, G. R. Whittell, L. De Cola, I. Manners, *Chem. Commun.* **2015**, *51*, 15921 – 15924.
[19] W. Zhang, W. Jin, T. Fukushima, T. Mori, T. Aida, *J. Am. Chem. Soc.* **2015**, *137*, 13792 – 13795.
[20] W. Zhang, W. Jin, T. Fukushima, A. Saeki, S. Seki, T. Aida, *Science* **2011**, *334*, 340 – 343.
[21] B. L. Feringa, R. A. van Delden, *Angew. Chem. Int. Ed.* **1999**, *38*, 3418 – 3438; *Angew. Chem.* **1999**, *111*, 3624 – 3645.
[22] M. M. Green, M. P. Reidy, R. D. Johnson, G. Darling, D. J. O'Leary, G. Willson, *J. Am. Chem. Soc.* **1989**, *111*, 6452 – 6454.
[23] B. M. W. Langeveld-Voss, R. J. M. Waterval, R. A. J. Janssen, E. W. Meijer, *Macromolecules* **1999**, *32*, 227 – 230.
[24] A. R. A. Palmans, J. A. J. M. Vekemans, E. E. Havinga, E. W. Meijer, *Angew. Chem. Int. Ed. Engl.* **1997**, *36*, 2648 – 2651; *Angew. Chem.* **1997**, *109*, 2763 – 2765.
[25] L. J. Prins, P. Timmerman, D. N. Reinhoudt, *J. Am. Chem. Soc.* **2001**, *123*, 10153 – 10163.
[26] E. Yashima, K. Maeda, H. Iida, Y. Furusho, K. Nagai, *Chem. Rev.* **2009**, *109*, 6102 – 6211.
[27] Y. Nagata, T. Yamada, T. Adachi, Y. Akai, T. Yamamoto, M. Suginome, *J. Am. Chem. Soc.* **2013**, *135*, 10104 – 10113.
[28] A. R. A. Palmans, E. W. Meijer, *Angew. Chem. Int. Ed.* **2007**, *46*, 8948 – 8968; *Angew. Chem.* **2007**, *119*, 9106 – 9126.
[29] V. K. Praveen, S. S. Babu, C. Vijayakumar, R. Varghese, A. Ajayaghosh, *Bull. Chem. Soc. Jpn.* **2008**, *81*, 1196 – 1211.
[30] M. Liu, L. Zhang, T. Wang, *Chem. Rev.* **2015**, *115*, 7304 – 7397.
[31] A. Ajayaghosh, R. Varghese, S. Mahesh, V. K. Praveen, *Angew. Chem. Int. Ed.* **2006**, *45*, 7729 – 7732; *Angew. Chem.* **2006**, *118*, 7893 – 7896.
[32] A. Lohr, F. Würthner, *Angew. Chem. Int. Ed.* **2008**, *47*, 1232 – 1236; *Angew. Chem.* **2008**, *120*, 1252 – 1256.
[33] J. van Gestel, *Macromolecules* **2006**, *39*, 1664 – 1664.
[34] J. van Gestel, A. R. A. Palmans, B. Titulaer, J. A. J. M. Vekemans, E. W. Meijer, *J. Am. Chem. Soc.* **2005**, *127*, 5490 – 5494.
[35] X. Ma, Y. Zhang, Y. Zhang, C. Peng, Y. Che, J. Zhao, *Adv. Mater.* **2015**, *27*, 7746 – 7751.

Received: March 21, 2016
Revised: May 16, 2016
Published online: June 29, 2016

